Supplementary Materials

Supplementary Figure 1.

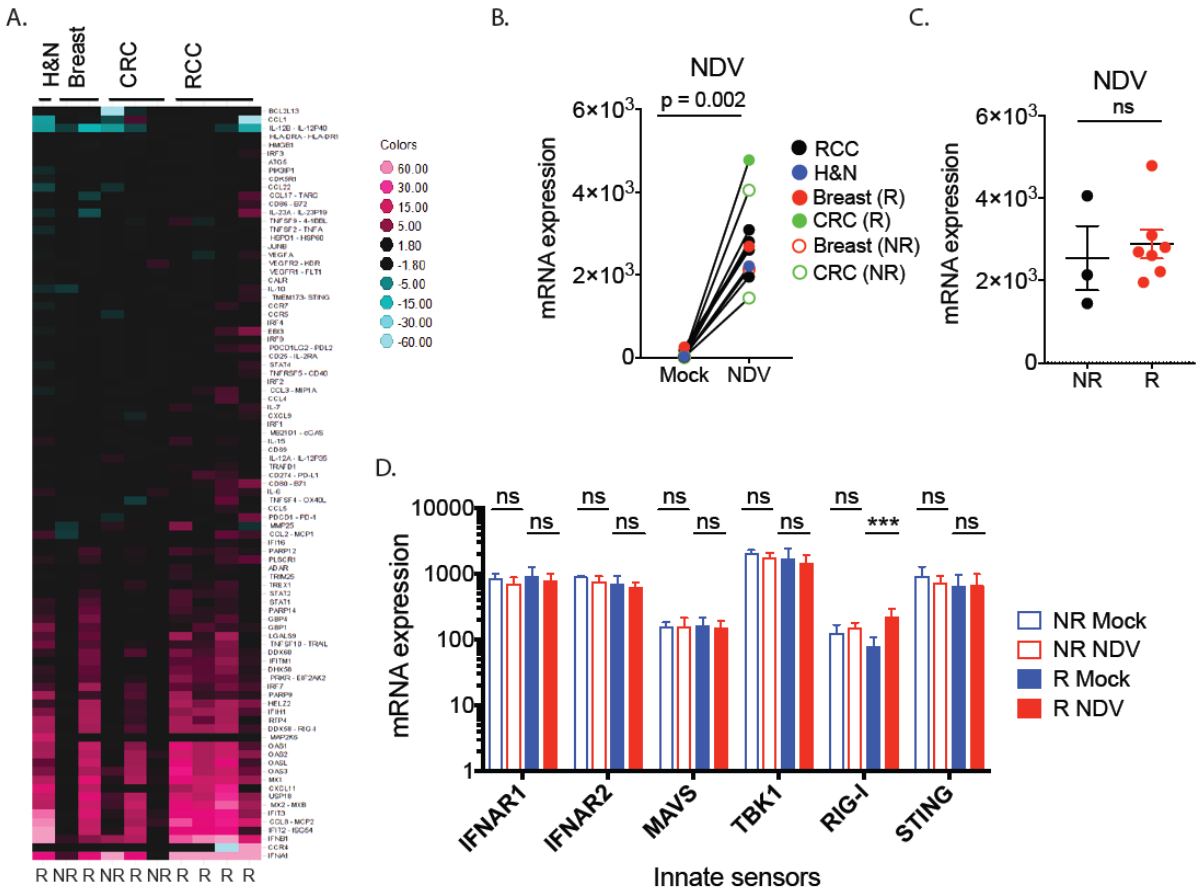

Supplementary Figure 1. Induction of immune-related gene and protein expression in human tumor histoculture samples following ex vivo treatment with NDV. Four renal cell carcinoma (RCC), 3 colorectal cancer (CRC), 2 breast cancer and 1 head and neck squamous cell carcinoma (HNSCC) tumor specimens were treated with NDV (3×10^7 pfu) for 24h. Following incubation, tissue samples were collected for gene expression analysis and supernatants were collected for cytokine detection. A. The heat map shows the fold change of the indicated genes with NDV treatment over media alone. R: NDV-responsive tumor. NR: NDV-nonresponsive tumor. B. Expression of NDV RNA in all tumors. C. Relative expression of NDV RNA in NDV-responsive (R) and non-responsive (NR) tumors. D. Expression of type I IFN receptor and innate sensor genes in NDV-responsive (R) and non-responsive (NR) tumors. Data were analyzed using Wilcoxon matched-pairs signed rank test (B), and Student's t tests for individual comparisons (C,D) ***$p<0.001$, ns: nonsignificant.

Supplementary Figure 2.

Supplementary Figure 2. Induction of immune-related gene and protein expression in plasma following ex vivo treatment of human whole blood with NDV for 24h. Whole blood (4 mL (a), 1ml (b)) from patients with solid cancers (n = 5) and normal healthy donors (n = 5) were untreated (media) or treated with 1.2×10^8 pfu NDV for 24 hours. The heat map shows the fold change of the indicated genes with NDV treatment over media alone.

Supplementary Figure 3.

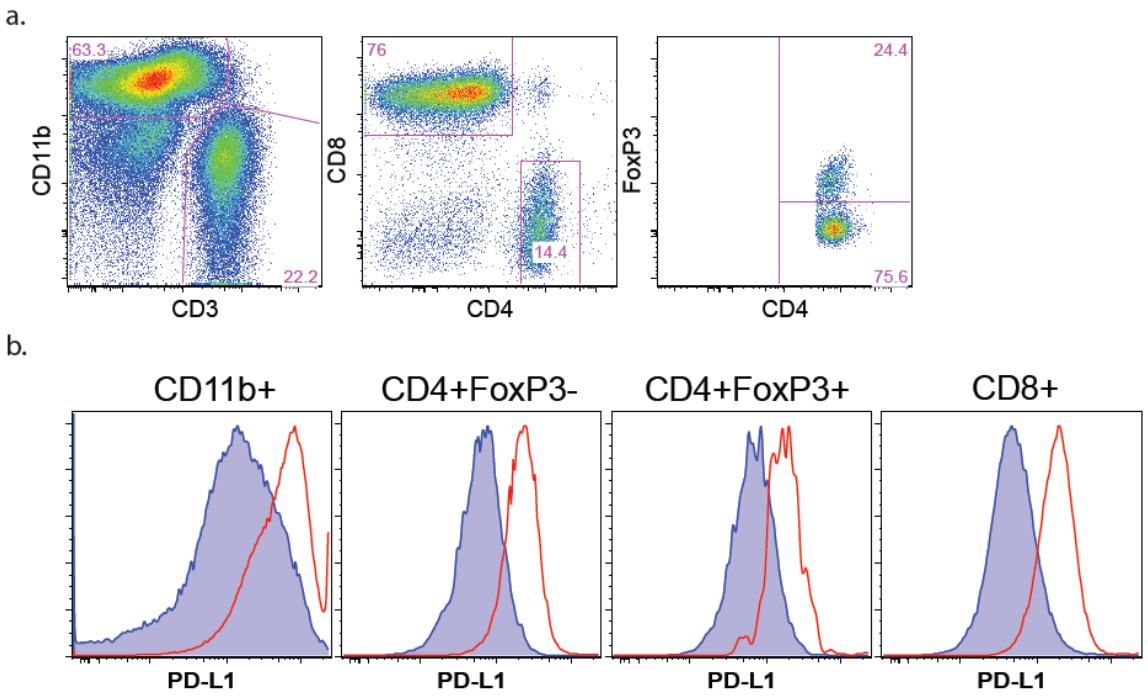

Supplementary Figure 3. Upregulation of PD-L1 on tumor-infiltrating leukocytes with NDV therapy. Animals were treated as specified in figure 2. a) Gating strategy for various leukocyte populations. b) Representative histograms of PD-L1 expression (blue: PBS-treated, red: NDV-treated). Data are representative of 2 independent experiments with 5 mice per group.

Supplementary Figure 4.

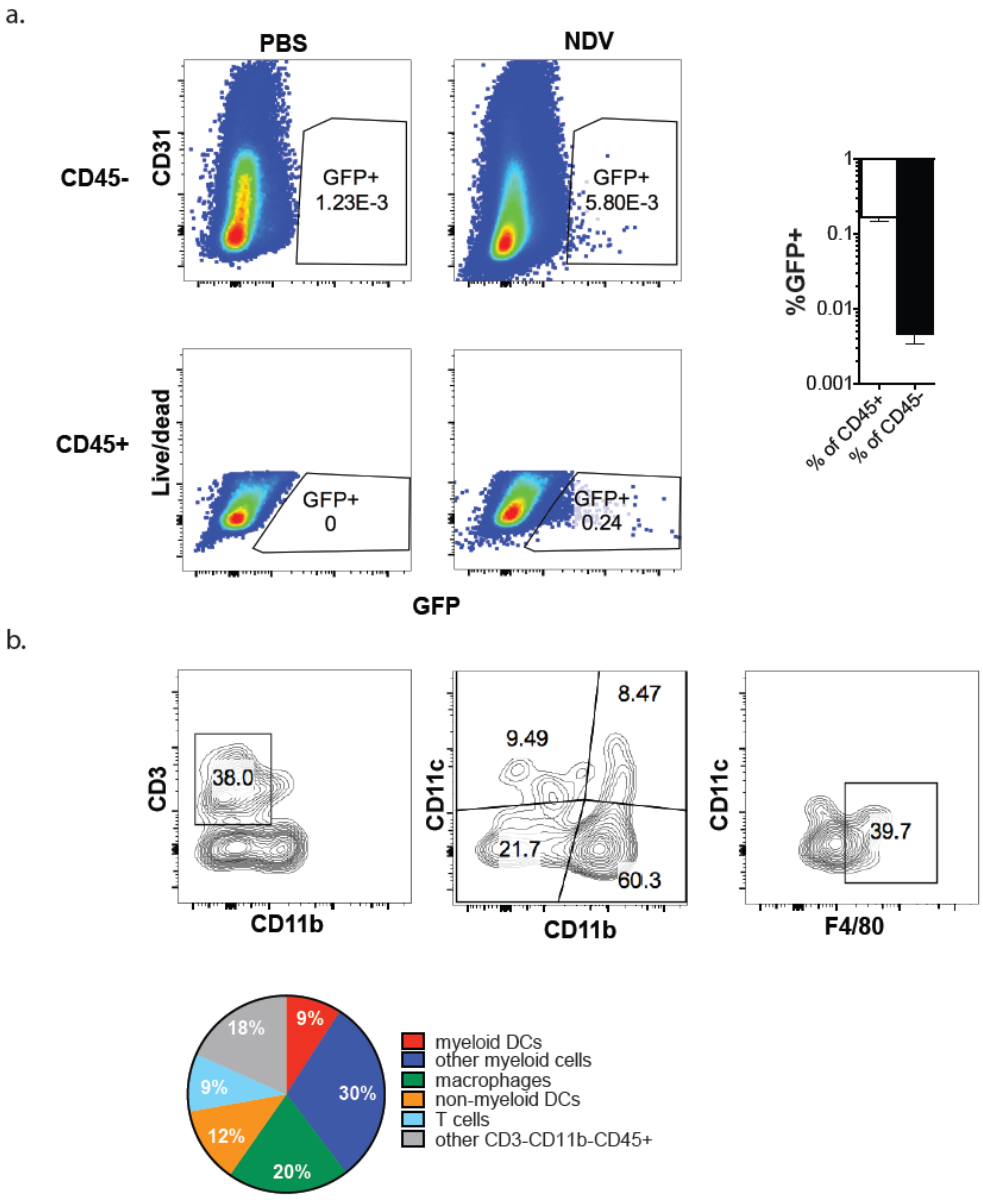

Supplementary Figure 4. NDV infection is restricted to minority of cells in tumor. B16-F10 tumor-bearing mice were treated intratumorally with NDV-expressing GFP, according to the schedule specified in figure 2. Tumors were excised 24 hours later and analyzed for GFP expression in various tumor cell populations. a) GFP expression in CD45- and CD45+ subsets. Left: representative histograms. Right: average calculated percentages. b) GFP expression in various leukocyte subsets. Top: representative histograms. Bottom: average calculated percentages. Individual leukocyte subsets in GFP+CD45+ fraction were defined as follows: CD11b+CD11c+: myeloid DC's; CD11b+F4/80+: macrophages; CD11b-CD11c+: non-myeloid DC's; CD11b+CD11c-F4/80-: other myeloid cells; CD11b-CD3+: T cells. Data are representative of 2 independent experiments with 5 mice per group.

Supplementary Figure 5.

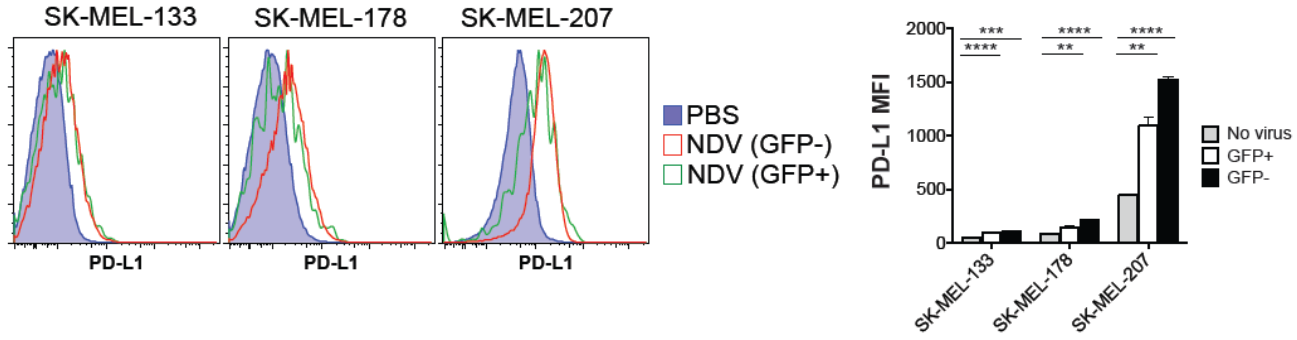

Supplementary Figure 5. Upregulation of PD-L1 on human melanoma cell lines.
Cell lines in culture were infected with NDV-GFP at MOI of 1 and at 24 hours the cells were isolated and analyzed for surface PD-L1 expression in GFP+ and GFP- fractions. Data are representative of 3 independent experiments with 3 replicates per group. Statistical significance was calculated using Student's t tests. **p<0.01, ***p<0.001, ****p<0.0001

Supplementary Figure 6.

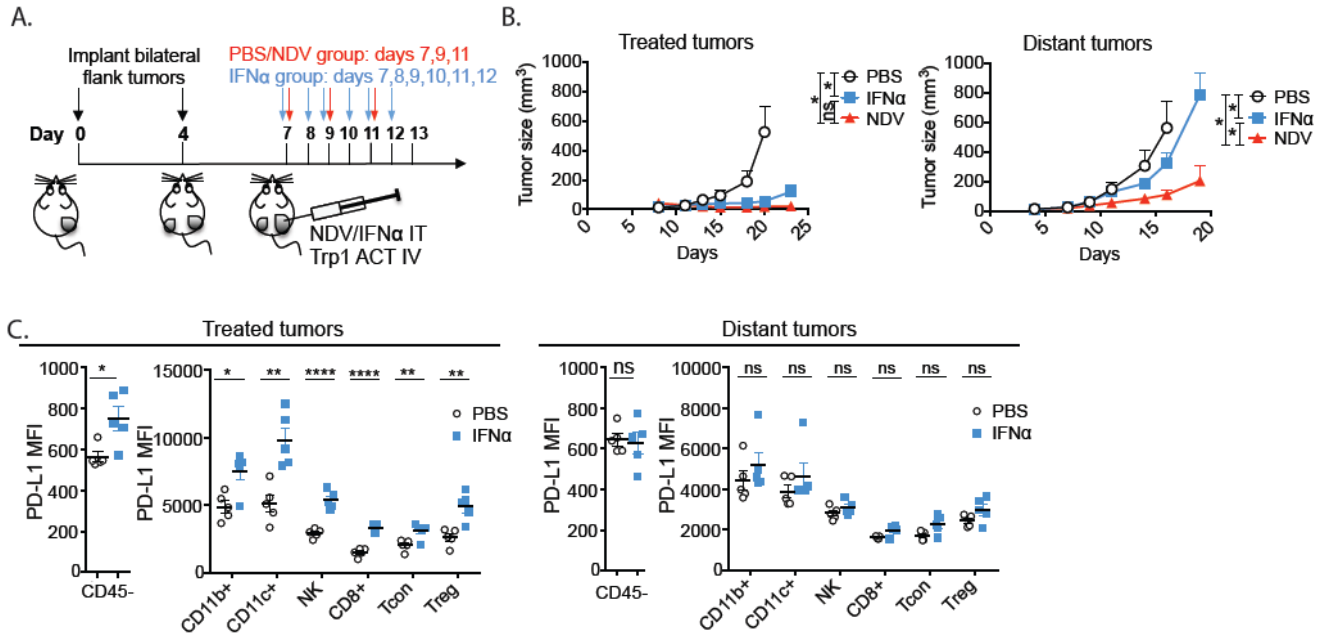

Supplementary Figure 6. Type I IFN provides local, but not distant tumor control and PD-L1 upregulation. A) Treatment schema. B) Growth of treated and distant tumors. C) Upregulation of PD-L1 in the IFNα-treated and distant tumors in CD45$^-$ compartment and individual leukocyte subsets. Data demonstrate representative results from 2 independent experiments with 5-10 mice per group. Data demonstrate representative results from 2-3 independent experiments with 5-10 mice per group. (B) Statistical significance was calculated using ANOVA with multi-group comparisons using tumor sizes at day 20 (treated tumors) and day 16 (distant tumors). (C) Statistical significance was calculated using Student's T tests. *p<0.05, **p<0.01, ****p<0.0001, ns: non-significant. MFI: median fluorescence intensity.

Supplementary Figure 7.

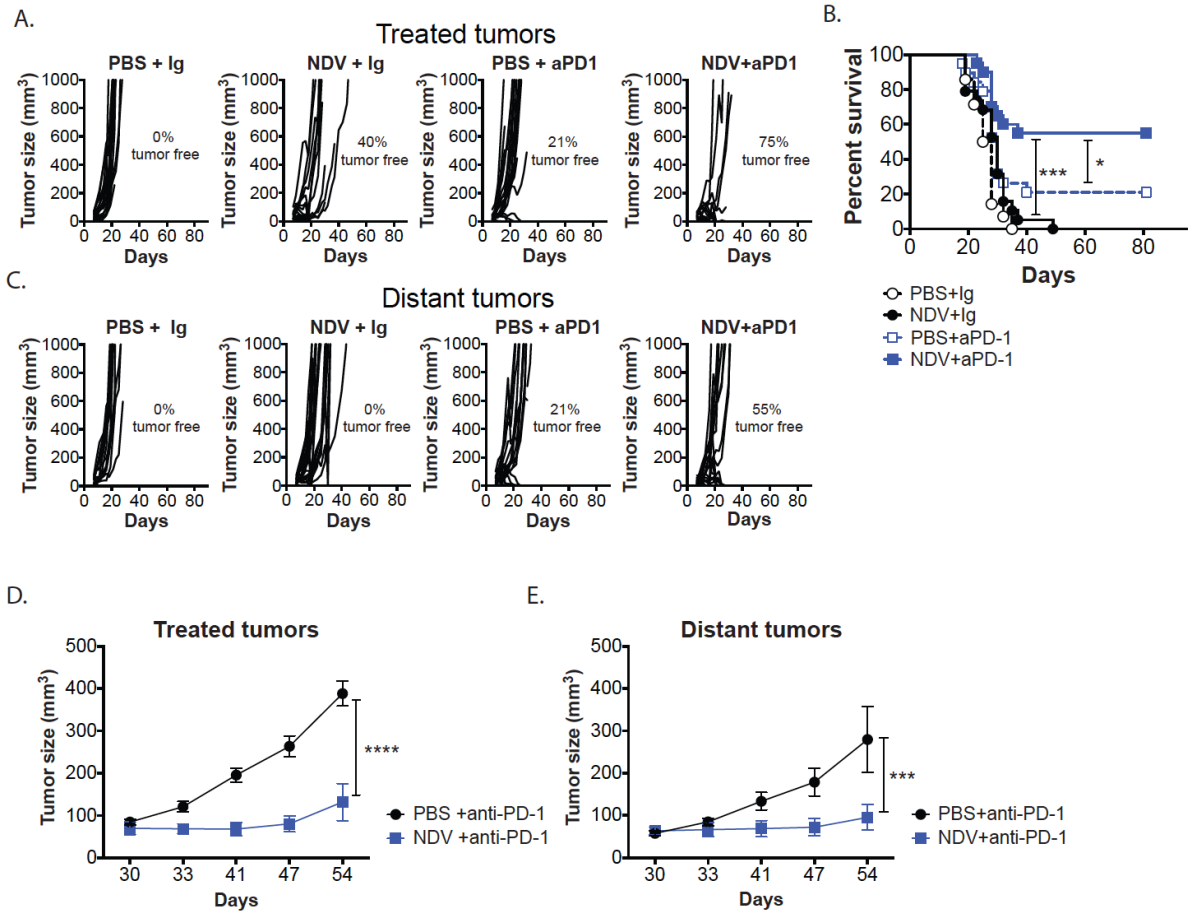

Supplementary Figure 7. Local and abscopal therapeutic effects in mouse tumor models treated with combination of intratumoral NDV with systemic PD-1 blockade.
a-c) CT26 colon carcinoma model. $5x10^5$ cells were implanted in the right and left flank on day 0. Treatment was performed on days 7, 9, 11, and 13 with concomitant intraperitoneal anti-PD-1 antibody or isotype control. a) Growth of NDV-treated CT26 tumors. b) Growth of distant CT26 tumors. c) Overall survival in the CT26 model. Data represent pooled results from 2 independent experiments with 5-10 mice per group. d-e) Inducible $BRAF^{V600E}$-$PTEN^{loxP/loxP}$ mouse melanoma model. Tumors were induced by tamoxifen painting on bilateral flanks. Animals bearing established bilateral flank tumors were treated intratumorally into the right tumor with PBS or NDV in combination with IP anti-PD-1 antibody starting on day 30 after tumor induction. c) Growth of NDV-treated tumors. d) Growth of distant tumors. Data demonstrate representative results from 1 of 2 independent experiments with 5 mice per group. Statistical significance was calculated using log-rank test (B) and Student's T tests (D-E). *p<0.05, ***p<0.001, ****p<0.0001.

Supplementary Figure 8.

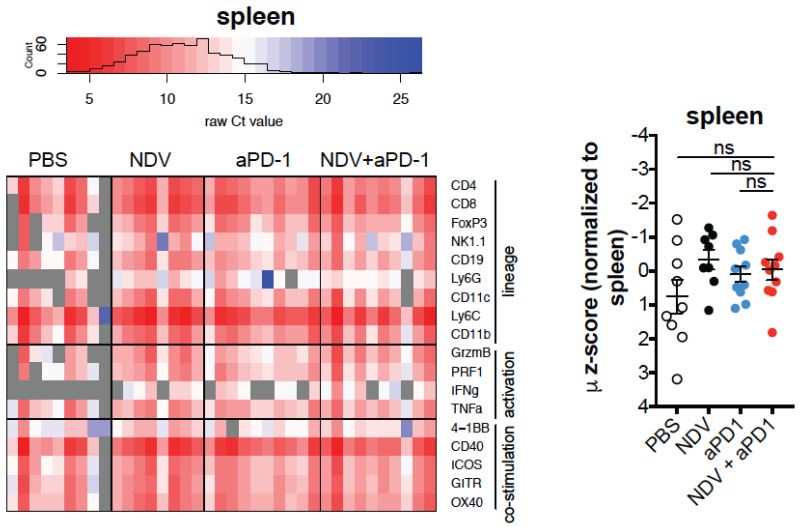

Supplementary Figure 8. Gene expression analyses from spleens of animals treated with NDV and anti-PD-1 therapy.

Animals were treated as per Figure 7. Spleens from the treated animals were excised on day 15 and processed for gene expression analysis using Fluidigm focusing on selected lineage-defining markers and T cell activation and co-stimulatory markers. Co-stimulation and activation markers were used to calculate an activation signature z-score displayed in the panels to the right of the heatmap. Data represent 1 experiment with 10 mice per group. Statistical significance was calculated using ANOVA with multiple comparisons. ns: non-significant.

Supplementary Figure 9.

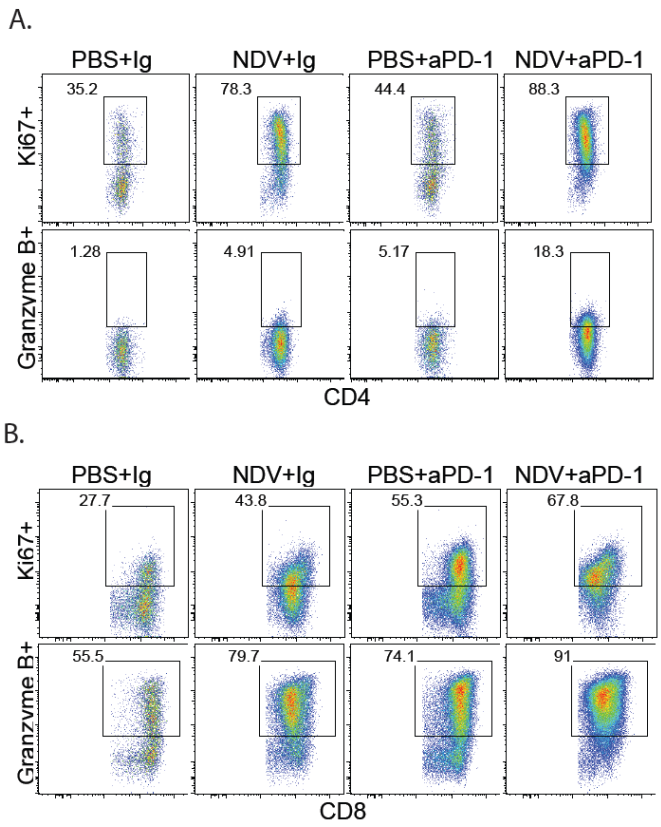

Supplementary Figure 9. Upregulation of proliferation and lytic markers in lymphocytes from distant tumors in response to combination of NDV with PD-1 blockade.
Animals were treated as per Figure 7. a) Expression of Ki67 and Granzyme B by tumor-infiltrating CD4+FoxP3- lymphocytes. b) Expression of Ki67 and Granzyme B by tumor-infiltrating CD8 lymphocytes. Data represent 1 of 2 experiments with 10 mice per group.

Supplementary Figure 10.

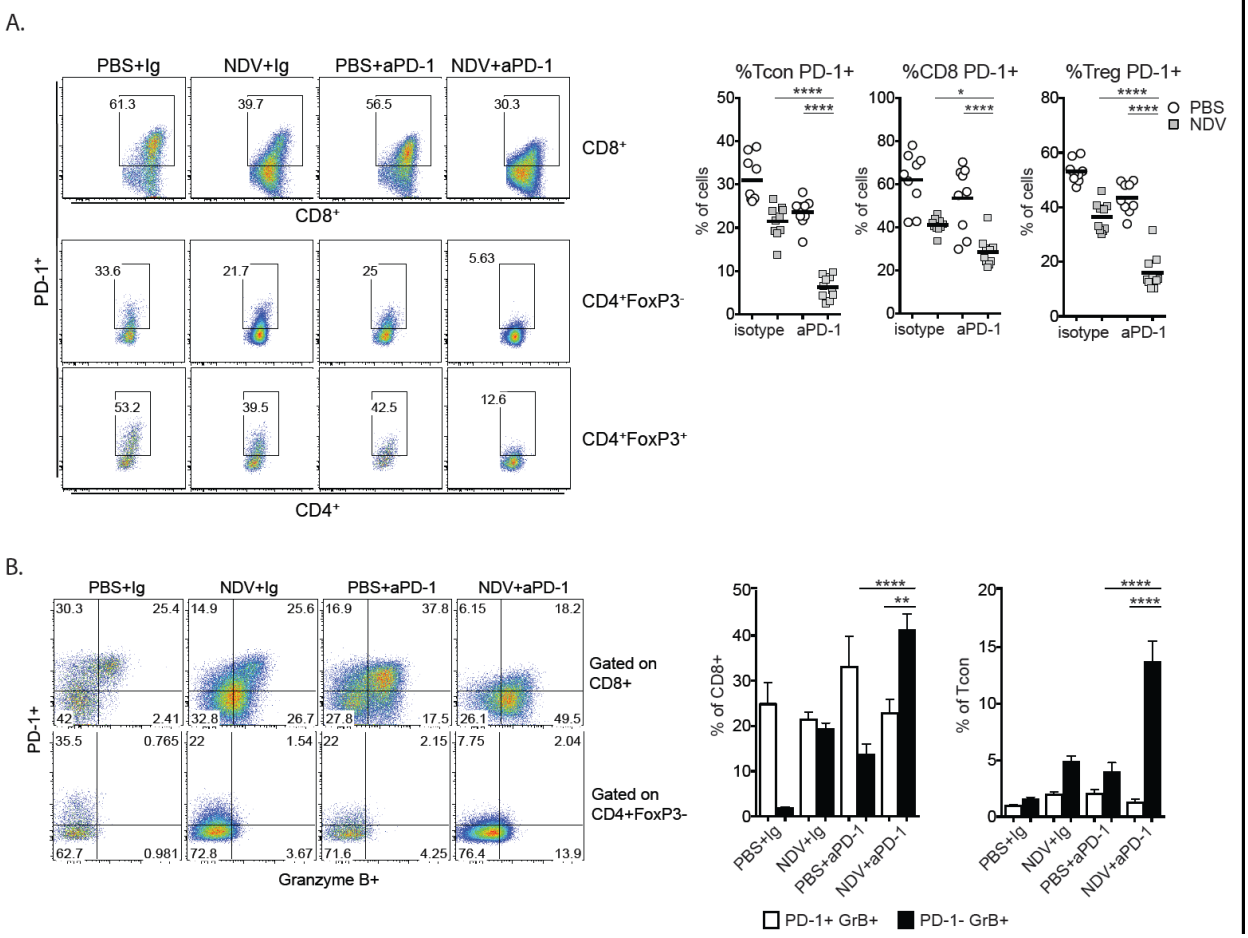

Supplementary Figure 10. T cells expanded with NDV+aPD-1 therapy exhibit activated phenotype. A) Surface PD-1 expression by distant tumor-infiltrating $CD8^+$, Tconvs, and Tregs. Left: representative flow cytometry plots. Right: grouped plot of all samples. B) Expansion of PD-1^-Granzyme B^+ $CD8^+$ lymphocytes in distant tumors. Left: representative flow cytometry plots. Right: grouped plot of all samples. Statistical significance was calculated using ANOVA with multiple comparisons. Data represent 1 of 2 experiments with 10 mice per group. Statistical significance was calculated using ANOVA with multiple comparisons. *p<0.05, **p<0.01, ***p<0.001, ****p<0.0001, ns: non-significant.